Journal of Chromatography, 548 (1991) 127–145
Elsevier Science Publishers B.V., Amsterdam

CHROMSYMP. 2315

High-performance liquid chromatography of amino acids, peptides and proteins

CXII[a]. Analysis of operating parameters affecting the breakthrough curves in fixed-bed chromatography of proteins using several mathematical models

A. JOHNSTON, Q. M. MAO and M. T. W. HEARN*
Department of Biochemistry and Centre for Bioprocess Technology, Monash University, Clayton, Victoria 3168 (Australia)

ABSTRACT

Performance of a packed bed, in terms of adsorbent utilization and kinetic characteristics, was studied for the adsorption of HSA to the ion-exchange resins, DEAE Trisacryl M and DEAE Sepharose FF. The influence of column length, temperature and feed concentration on the shape of the breakthrough curve has been investigated and the resulting operating capacities, q^* measured by graphical integration. Mathematical models prevalent in the literature have been used to extract out the kinetic parameters, the effective diffusivity, D_p, and the interaction rate constant, k_1, from the experimental breakthrough curves, and these parameters have been used to evaluate the performance of the columns and to validate the models selected. The effect of protein size on the adsorption behaviour was also investigated using the proteins HSA, transferrin and ferritin, determining q^*, k_1, and D_p from the breakthrough curves.

INTRODUCTION

Chromatographic separation of proteins relies upon the differential rates of solute migration encompassing relative retention characteristics throughout a packed bed. In such systems, complex mixture of proteins can be separated on the basis of biophysical differences, such as apparent ionic charge (ion-exchange chromatography), hydrodynamic size (gel filtration), hydrophobicity (reversed-phase chromatography, hydrophobic interaction chromatography), as well as on the basis of functional differences, utilizing their preferential affinities for biospecific and biomimetic adsorbents (affinity chromatography).

On a preparative scale, large volumes of a fermentation broth or a biological fluid are required to be processed to extract the protein of interest. In process

[a] For Part CXI, see ref. 36.

0021-9673/91/$03.50

applications, the feed is often continually loaded down a packed chromatographic bed, the upper part of the bed, at the feed entrance, selectively adsorbing the proteins in order of their respected affinities and diffusivities. Protein left in the bulk solution is substantially removed by the lower layers of the adsorbent, near the exit, and the effluent becomes essentially protein depleted, as illustrated by the curve shown in Fig. 1 (position a). At some time later the bed becomes saturated, the proteins appear in the effluent (position b) and the bed is then said to have reached the breakthrough point. Protein concentration in the effluent continues to rise until the outlet concentration reaches the value of the inlet concentration (see Fig. 1, position c). The concentration profile emerging from the bed is termed the breakthrough curve. This type of

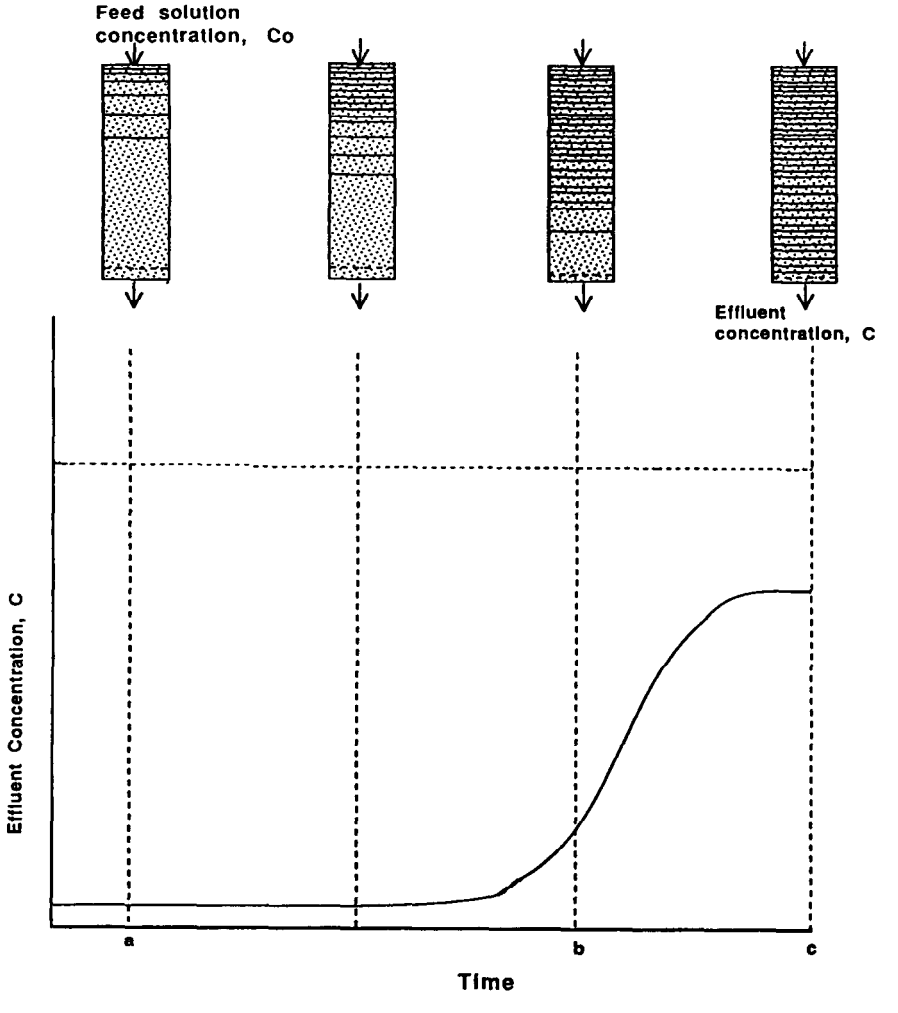

Fig. 1. Schematic representation of the adsorption of a protein solution to a resin in a packed bed, progressing as bands, or adsorption zones, with the effluent concentration profile (breakthrough curve) emerging from the packed bed.

preparative loading (frontal chromatography) is in direct contrast to analytical zonal chromatography, where the sample to be separated is injected in small quantities as a pulse onto the top of the column.

Breakthrough curves represent important profiles of the processes which are occurring down the chromatographic bed. Two characteristics of these breakthrough curves are important in assessing the performance of the bed: firstly, the position of the breakthrough curve which depends *inter alia* on the operating capacity of the adsorbent, and secondly the shape, which can be indicative of the interaction kinetics of the protein. In preparative chromatography, feed loading is usually terminated when the protein concentration in the effluent exceeds a certain amount. This choice is made to maximize the capacity of the adsorbent and minimize the amount of protein lost in the effluent. A steep breakthrough curve is therefore desirable. Thus, with knowledge of the adsorbent's capacity and its adsorption kinetics, the operating performance of the system can be optimized. This optimization becomes increasingly more important in preparative biochromatography where high productivity and high yield of product are paramount.

This study then represents an initial cross-examination of some of the factors thought to influence adsorption behaviour of ion-exchange adsorbents in process biochromatography. The parameters studied include the column length, temperature and feed concentration, as well as the effect of the size of the protein, and were selected to assess their effects on the breakthrough curves. Graphical integration and mathematical models found in the literature were also used to extract out physico-chemical parameters governing the adsorption process, from the experimental profiles emerging from the operation of packed bed chromatographic systems.

THEORY

Equilibrium parameters of an ion-exchange resin

For a packed bed, operating at constant flow-rate, the operating capacity can be calculated by graphical integration as seen by the relationship,

$$q^* = \int_{V=0}^{V_f} \frac{[C_0 - C(t)]\mathrm{d}V}{V_c} \tag{1}$$

where q^* = protein concentration bound to the resin in equilibrium with C_0; C_0 = feed concentration, inlet concentration; $C(t)$ = protein concentration in the effluent at any time, t; V = volume of feed passed through the column; V_c = volume of the chromatographic bed; V_f = total volume passed. This graphical treatment is applicable to high interaction rates, and is based on the concept that interaction occurs within an adsorption zone that descends through the packed bed, see Fig. 1.

Analysis of the shape of the curve can be initially based on visual examination. If the adsorption process was infinitely rapid, the curve would appear as a sharp rectangular front. However, in many situations a sigmoidal shape is commonly seen which is the result of a complex interplay of equilibrium and non-equilibrium processes occurring during adsorption. The curve may be steep or relatively flat or in some cases

considerably distorted [1] as a consequence of inadequate fluid mixing along the bed, slow kinetics of adsorption, slow diffusion of the protein, non-specific adsorption or conformational changes of the protein. The steepness, or slope, of the profile can be estimated from measurements of the "spread" of the curve, which is determined by the difference between the volume throughput at 10% saturation (V_{10}) and the volume throughput at 90% saturation (V_{90}). For ideal, infinitely fast adsorption, the breakthrough curve is a sharp front, the spread is minimal, and thus the difference between V_{10} and V_{90} is zero.

Mathematical models

A quantitative analysis of the non-equilibrium effects contributing to the shape of the breakthrough curves is only possible if the chromatographic process can be described in physical terms based on mathematical solutions. In this context, the concept of a theoretical model (from the word "modus", a measure) implies that the process can be described by a set of equations which reflect the physical reality of the adsorption and mass transport events. Mathematical descriptions of adsorption processes in biochromatography first gained prominence in the 1940's, when the local equilibrium model was developed. The adsorption behaviour was derived from purely thermodynamic considerations, yielding equilibrium isotherms that were based on either a constant separation factor (for example the Freundlich isotherm), the Langmuir equation or simply empirical relationships. Martin and Synge [2] put forward the plate theory, directly relating adsorption chromatography in a fixed bed to fractional distillation and extraction processes. According to the plate theory, the chromatographic bed consists of a number of theoretical plates, and within each plate local equilibrium was established between the mobile and stationary phases. Diffusion between the plates was assumed negligible. The equilibrium relationship between the two phases was a linear one, with the distribution ratio being independent of the concentration of the solutes. The plate theory has been widely used in analytical zonal chromatography to predict peak positions and widths [3,4] but has limited application in preparative chromatography, where the interaction between the solutes and the phases is no longer a simple linear first order process, that is, overloaded conditions may apply.

Although simple in concept and computation, these numerical solutions derived from the plate theory also provide little insight to the understanding of the dynamics of adsorption. It must be remembered that the adsorption of a protein to an adsorbent is a dynamic process: local equilibrium will rarely be achieved in this flowing system, partly because it takes time for the protein to reach the surface of the adsorbent, and partly because diffusion inside a porous adsorbent can be comparatively slow. Obviously, the slower the fluid flow and the larger the pores of the adsorbent, the more complete the process approaches the near-equilibrium criterion.

If the process is seen then, as a series of mass transfer mechanisms operating at or near equilibrium, the mathematical equations become a complex set of partial differential equations, too complex as yet to solve analytically. Other approaches to modelling this dynamic process have therefore been concerned with simplifying the equations, by assuming that one mass transfer mechanism predominantly controls the adsorption, see Golshan-Shirazi and Guiochon [5] for an extensive review. For example, Hubble [6] describes a simple model in which all the mass transfer resistances

except the rate of interaction have been neglected, and the mathematical equations are solved in discrete stages down the column bed. Applying it here to ion-exchange adsorption of protein, the model of Hubble gives the concentration of protein adsorbed to the resin as,

$$q = \frac{(b - \sqrt{x})(2k_1q_0 + b + \sqrt{x}) - (b + \sqrt{x})(2k_1q_0 + b - \sqrt{x})e^{(t\sqrt{x})}}{2k_1[e^{(t\sqrt{x})}(2k_1q_0 + b - \sqrt{x}) - (2k_1q_0 + b + \sqrt{x})]} \quad (2)$$

where $x = (b^2 - 4k_1^2C_{0i}q_m)$; $b = -(k_1C_{0i} + k_1q_m + k_2)$; C_{0i} = inlet concentration of stage i; k_1 = forward rate constant; k_2 = reverse rate constant; q = concentration of adsorbed protein at any time, t; q_m = maximum protein capacity of the adsorbent; q_0 = initial concentration of protein adsorbed at each stage.

Thomas [7] devised an analytical solution to the mass balance equations that describe fixed bed ion-exchange adsorption for small solutes and fixed bed gas adsorption. The solution is based on a second order rate of exchange, assuming all other mass transport resistances are negligible. When applied to protein adsorption to ion-exchange sorbents, the concentration emerging from the column can be calculated from the sigmoidal relationship,

$$\frac{C(t)}{C_0} = \frac{J(n/r,nT)}{J(n/r,nT) + [1 - J(n,nT/r)]\exp[(1 - 1/r)(n - nT)]} \quad (3)$$

where $r = 1 + C_0/K_d$; $n = q_mk_1z/u_0$; $T = [u_0(K_d + C_0)/(zq_m)](t - z\varepsilon/u_0)$; $K_d = k_2/k_1 = 1/K_a$; ε = bed voidage; J = the integral of the Bessel function; u_0 = superficial velocity; z = column length, bed height.

Arnold *et al.* [8] have argued that with porous particles the rate at which protein diffuses into the interior is likely to be significant. In fact, it is conceivable that if the protein to be purified has a large hydrodynamic radius and the pore openings of the sorbent are small, mass transfer of the protein will be reduced due to the geometric restraints placed upon its movement into the pores. Arnold *et al.* in development of their model equations, have visualized the mass transfer steps as a number of transfer units each acting in series. Their simplified solution is based on the assumption that the effect of axial dispersion is small and that the rate of adsorption is infinitely fast compared to the effects of pore diffusion. The equation for the breakthrough curve takes the form,

$$T\text{-}1 = \left(\frac{1}{N_{pore}} + \frac{1}{N_f}\right)\left[\phi(X) + \frac{N_{pore}}{N_f}(\ln X + 1)\right]\left(\frac{N_{pore}}{N_f} + 1\right)^{-1} \quad (4)$$

where $\phi(X) = 2.44 - 3.66\sqrt{1 - X}$; $X = C(t)/C_0$; $T = (V - \varepsilon v)/(\rho_b q^* v/C_0)$; $N_{pore} = 15D_p(1 - \varepsilon)z/r_p^2u_0$; $N_f = K_fa_pz/u_0$; a_p = external surface area of the adsorbent per unit volume of the bed; $C(t)$ = concentration of protein in solution at any time; t; D_p = effective (pore) diffusivity; K_f = film mass transfer coefficient; q^* = equilibrium concentration of protein adsorbed; ρ_b = bulk density of the adsorbent; v = volume of the adsorbent.

For cases where the equilibrium relationship is no longer a linear one, and more than one mechanism is proposed to operate, the interrelated equations become too complex for an exact, analytical solution, and numerical computation offers the only practical solution. Vermeulen [9] has outlined a solution to the mass balance equations using an empirical approximation to the finite series arising from the equations. Fleck *et al.* [10] used the finite difference method of Crank and Nicholson, basing their solution on a constant flow pattern, and assuming a dominantly slow interaction rate of mass transfer within the adsorbent. Katoh *et al.* [11] use this same technique to evaluate the breakthrough curve from the adsorption of trypsin to the affinity adsorbent, Sepharose 4B-STI. Garg and Ruthven [12] also used this technique for describing the micro-diffusion during molecular sieving. Orthogonal collocation techniques are also gaining popularity, despite the fact that the large grid system necessary for an accurate solution often renders long computational times. Some investigators have solved the equations by collocation techniques using various equilibrium relationships. For example, Tien and Thodos [13] have derived solutions for favourable Freundlich isotherm, Morton and Murni [14] for an empirical non-linear relationship, whilst Antonson and Dranoff [15] have applied these techniques to the Langmuir isotherm. These investigators [13–15] have all assumed that intraparticle diffusion is the rate controlling mechanism, thus reducing the complexity of their numerical solutions. Also using orthogonal collocation techniques, Arve and Liapis [16] have incorporated three rate controlling mechanisms, that is, resistances due to pore diffusion, film diffusion and the dynamics of the interaction step, into a computational solution for the breakthrough profile. The fundamental mass balance equation from which their solution is derived takes the form.

$$D_a \frac{\partial^2 C(t)}{\partial x^2} - \frac{u_0}{\varepsilon} \frac{\partial C(t)}{\partial x} = \frac{\partial C(t)}{\partial t} + \left(\frac{1-\varepsilon}{\varepsilon}\right) \frac{\partial q}{\partial t} \tag{5}$$

where D_a = axial diffusivity; x = distance down the bed. The overall rate of change of the amount of protein adsorbed to the sorbent, $(\partial q/\partial t)$, is dictated by various mass transfer coefficients and surface interaction rates. As yet there is no exact solution to eqn. 5. There are, however, conditional solutions provided that certain terms are neglected or that fixed values (sometimes unreasonable) are chosen for the boundary conditions. Eqns. 2–4 represent these conditional solutions. Unconditional solutions arise from numerical techniques, such as those developed by Arve and Liapis. Despite the inherent pitfalls of numerical, brute-force solutions, particularly with respect to numerical instability, and lengthy computational time, the solution of Arve and Liapis, represents the most advanced treatment yet available for the quantification or prediction of the adsorption behaviour of proteins. Neglecting the axial diffusion term, D_a, in eqn. 5, the numerical solution is described by Arve and Liapis [16] and is referred to hereafter in conjunction with eqn. 5.

It is important to recognise that each mass transfer resistance may affect the efficiency of the adsorption process to a different extent, and thus subtle differences may be evident in the pattern of the breakthrough curves emerging from the packed bed. This can be seen most clearly in a pictorial representation, as shown in Fig. 2, which compares theoretical profiles for the chemical adsorption process of small solutes under non-linear conditions, taken from mathematical model solutions

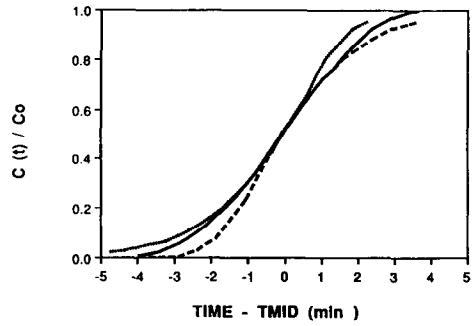

Fig. 2. Theoretical breakthrough curves for a Langmuir equilibrium equation, for different rate controlling mechanisms. The time is taken from the moment when enough liquid has passed through to displace the column dead volume and TMID corresponds to the time at 50% breakthrough, the midpoint. ····· = Fluid film; ——— = pore diffusion and – – – = solid film.

outlined in the literature [17]. For a particular set of operating conditions, the differences between the curves generated from either a pore diffusion model, a solid film resistance model or a liquid film resistance model are significant, and the greatest difference is seen at the initial time region. Thus, if a film diffusion model were to be used when pore diffusion restrictions were significant, large errors in predicting the dynamic capacity could occur. To further emphasize the differences in the theoretical predictions of the breakthrough curves incurred from different models, Fig. 3 compares the breakthrough curves derived from the models used in this investigation and outlined above. The models of Hubble [6] and Thomas [7] assume that the adsorption is controlled by the rate of interaction, Arnold *et al.* [8] assume the rate limiting step is pore diffusion, whilst Arve and Liapis [16] include three rates; an interaction rate, pore diffusion and a film coefficient. The curves of Fig. 3 were derived for a given set of conditions, $k_1 = 0.01$ mg/ml s and $D_p = 6.1 \cdot 10^{-11}$ m^2/s, and for these conditions the models of Hubble and Thomas give nearly identical curves as expected. For the same k_1, the model of Arve and Liapis predicts a shallower curve. This is because the model

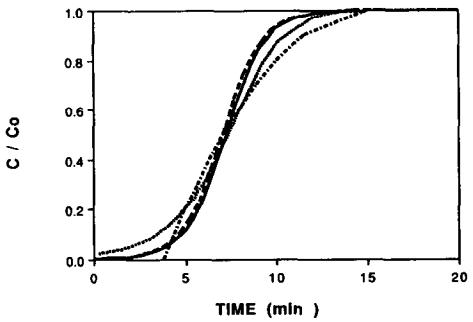

Fig. 3. Comparison of the theoretical solutions based on the adsorption of human serum albumin to DEAE Trisacryl M. ——— = Hubble [6]; – – – = Thomas [7]; – · – = Arnold *et al.* [8] and ····· = Arve and Liapis [16]. $C_0 = 1.5$ mg/ml, $q_m = 20$ mg/ml resin, $K_a = 56$ ml/mg, $u_0 = 0.042$ cm/s, $z = 1.3$ cm, $K_f = 8 \cdot 10^{-6}$ m/s, $k_1 = 0.01$ ml/mg s.

of Arve and Liapis includes not one but three independent rate constants, and thus the overall resistance, which is proportional to the sum of the reciprocal of each of these constants, will be higher. A higher overall resistance will therefore render a shallower breakthrough curve. In other words, if one were to fit a particular experimental curve, the best correlated value of k_1, computed from the model of Hubble or Thomas, will be low or a slow rate. The model of Arve and Liapis, will give a higher k_1 value, or a faster rate, which will be a closer approximation to the true rate of interaction.

When simplifying assumptions are used to reduce the mass balance equations from an intractable, complex form into something more manipulative, the question then should be raised as to what the physical consequences are. Have these assumptions any relation to the treatment of the experimental data? Are the assumptions physically valid?

In spite of the limitations of the models outlined above, each has contributed further towards understanding the adsorption process with biopolymers. Which model to select to adequately characterise the process at hand depends on the complexity of the feed stock, the integrity of the target protein and the homogeneity of the adsorbent's micro- and macro-structure. Moreover, the model may satisfy the necessary conditions to provide an adequate description of the overall experimental mass transfer resistances but not provide a sufficient condition to allow discrimination of the individual kinetic events [5,18]. However, most important is whether the selected model provides practical guidelines for the scale-up of the purification at the plant level. Such a selection may in fact use a model which does not precisely reflect the physical realities of the adsorption process. Equally relevant is the need for more precise physical models with extensive data bases which simulate more adequately the experimental measurements. Even with the sophisticated mathematical processing packages which are currently available, long computational times are often required and these theoretical methods cannot as yet accommodate the simplest error function in process chromatography as practiced today —the inadvertent foibles of the plant operator.

The development of the heuristic and physical criteria which will allow the choice of a particular model remains an important and challenging task. The aim of this work was thus twofold. Experimental data has been generated to provide an examination of the parameters influencing the breakthrough curve, and hence the efficiency of the chromatographic column, with specific reference to the effect of column length, temperature, concentration and the pore to protein size ratio. These data have then been used to test the efficacy of four of the models discussed above. The solutions of Hubble (eqn. 2), Thomas (eqn. 3) and Arve and Liapis (eqn. 5) have been adapted to obtain the interaction rate constant, k_1, for several proteins to an anion-exchange sorbent, whilst the values for effective diffusivity, D_p, were extracted from the solutions of Arnold (eqn. 4) and Arve and Liapis (eqn. 5) for human serum albumin (HSA) with two different anion-exchange sorbents.

The effect of operating parameters

Van Deemter plots, showing the dependence of column efficiency, measured in terms of height equivalent to a theoretical plate (HETP) on the flow velocity are abundant in the literature [19,20]. The adverse effects of operating packed bed chromatographic systems at high flow velocities are clearly evident from such plots. To

obtain a small HETP and therefore an efficient separation process, uniform packing of the sorbent is essential with polydisperse particles. A significant loss of efficiency can incur through uneven size distribution of the adsorbent causing local variation in the bed voidage. Due to current limitations in packing technology, the problem of uneven packing becomes increasingly severe as the bed length and diameter increases, and this can then lead to maldistribution of the feed flow. These limitations result in shallow and distorted breakthrough curves. The length of the column has therefore been recognised as an important and influential parameter, and its effect on the breakthrough curve, and hence column efficiency has been addressed here.

Another parameter thought to influence process performance is temperature. It is known that an increase in temperature leads to a decrease in fluid viscosity, which will render an increase in the mobility, and hence diffusivity, D_m, of protein in solution (according to the correlation developed by Young *et al.* [21], $D_m \propto 1/(\mathrm{MW}\ T^{1/3})$. High diffusivities will in turn lead to better mixing and faster mass transfer. Yamamoto *et al.* [4] have shown that an increase in temperature decreases the HETP of an analytical chromatographic column. Davies *et al.* [22] have shown a greater capacity in the separation of bilirubin from albumin in ion-exchange chromatography, when the system is operated at high temperature. From a thermodynamic point of view, this observation is not surprising. If the process of protein adsorption to an ion-exchange resin is exothermic, an increase in temperature will favour an increase in capacity, q^*. Indeed, the Van't Hoff equation predicts an increase in the association constant reflecting the change in the strength of interaction.

The effect of feed concentration on the adsorption performance is also of interest. Chromatographic operation in the overload mode, that is, at high solute concentrations, has been demonstrated to improve the productivity of mass transport in a separation process [23,24]. Why this occurs has not yet been elucidated. On the other hand, it has been suggested that there is a dependency of protein diffusivity on concentration. At high solution concentrations (> 1 mg/ml) the protein may have less freedom to move about by Brownian motion because of the increased number of molecules in solution and because of possible lateral interactions with increasing amounts of protein bound to the resin. Lundstrom and Elwing [25] and Petropoulos *et al.* [26] have viewed the interaction of protein–protein and protein–adsorbent in terms of surface coverage. Petropoulos *et al.* illustrated that the binding capacity depends on the availability and the probability of a protein in solution finding an adsorbed protein without any nearest neighbours, and at high coverages the availability and the probability will be low and thus the lateral interactions will become more significant. Thus high feed concentrations may influence the adsorption behaviour and hence alter the shape of the breakthrough curve.

Restricted diffusion is also believed to affect the performance of an adsorbent, and result in elongated breakthrough curves. A protein of large molecular dimensions is therefore anticipated to experience geometric constraint as it adsorbs to the porous resin. Furthermore, the effective aperture of the pore openings will diminish very quickly as the large protein molecules bind. Because of these influences the effect of protein size on the physicochemical parameters, k_1 and D_p, has also been addressed here as part of the present investigations.

MATERIALS AND METHODS

HSA was supplied as a 21% solution from Commonwealth Serum Laboratories (C.S.L.) (Melbourne, Australia), human apotransferrin, and ferritin isolated from horse liver, were purchased from Sigma (St. Louis, MO, USA). Fresh protein solutions were prepared with buffer the day of experimentation. For HSA and ferritin a 20 m*M* sodium acetate–acetic acid, pH 5.2 buffer, was chosen, unless stated otherwise, whilst 20 m*M* Tris–HCl, pH 7.0 was needed to affect adsorption of apotransferrin. Buffer salts were obtained from Aldrich (Milwaukee, WI, USA). Two weak anion-exchange resins were used in the experiments. Pharmacia DEAE Sepharose Fast Flow (FF) was selected as being a resin widely used in industry and therefore likely to be subjected to the variation in operating parameters investigated in this work. DEAE Trisacryl M, purchased from Australia Chemical Company (Melbourne, Australia) was selected for studying the effects of pore-to-protein size because (i) of its high molecular cut-off (according to the manufacturer), (ii) of its narrow particle size distribution and (iii) it has been used with our previous results with good reproducibility.

Pharmacia 5/5 HR columns (0.5 cm I.D., 5 cm maximum column length) were packed with the ion-exchange resins, DEAE Sepharose FF and DEAE Trisacryl M, to a bed height of 1.1–4.5 cm. When studying the temperature effects the columns were immersed in a water bath, maintained at a constant temperature. The other

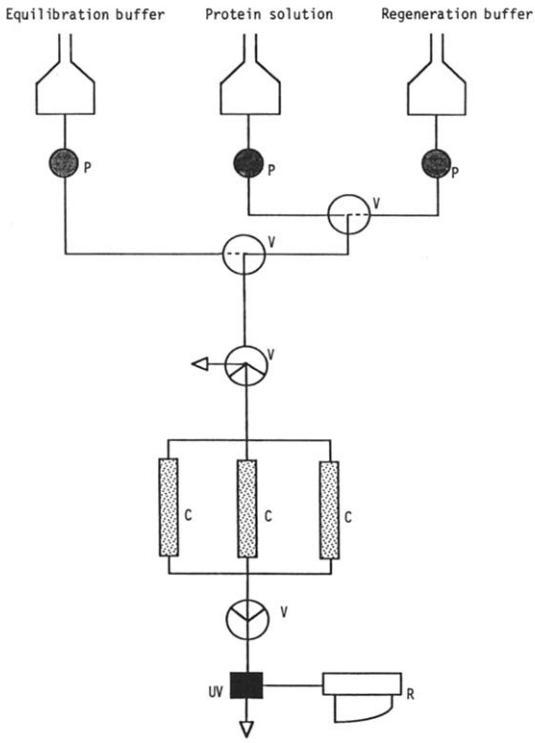

Fig. 4. Experimental set-up for fixed-bed configuration. P = Pump; UV = UV detector; V = valve; C = FPLC column and R = chart recorder.

experiments were carried out at room temperature. The columns were connected to a fast performance liquid chromatograph (FPLC) LC-500, from Pharmacia, that enabled automated and sequential loading, washing and elution of three identical columns. The effluent passed through a Model 1 UV Spectrophotometer, from Pharmacia (Uppsala, Sweden), which measured protein concentration at 280 nm, and this was linked to a two-pen chart recorder from Pharmacia for tracing the breakthrough curve. The experimental set-up is given in Fig. 4.

The protein concentrations were selected to ensure that the maximum capacity of the resin was attained so that overloaded conditions were maintained. These concentration levels were determined from the isotherms generated from batch experiments derived from our previous experiments [27,28]. Unless stated, a feed concentration of 1.5 mg/ml for HSA and transferrin and 0.1 mg/ml for ferritin was loaded onto the columns at a rate of 0.5 ml/min (u_0 = 0.042 cm/s).

The theoretical solutions of eqns. 2–5 were generated by computer programs written in PASCAL or FORTRAN on an IBM PC linked to a VAX mainframe. Graphical integration of the experimental breakthrough curves were also performed using the IBM PC.

Values for the film mass transfer coefficient, K_f, were taken from the correlation of Ohashi *et al.* [29] whilst the value for the mobile free diffusivity was calculated from the correlation given by Young *et al.* [21].

RESULTS AND DISCUSSION

Influence of column length, temperature, feed concentration and protein size on the capacity of the adsorbent and the shape of the breakthrough curve

Fig. 5 illustrates the change in the shape of the breakthrough curve for the adsorption of HSA to DEAE Trisacryl M with decreasing column length. Here it is clearly evident that the shorter the column, the sharper the profiles at the initial stages of adsorption. This observation concurs with the concept that in practical terms, with short columns consisting of preparative sorbents of broader particle diameter, the

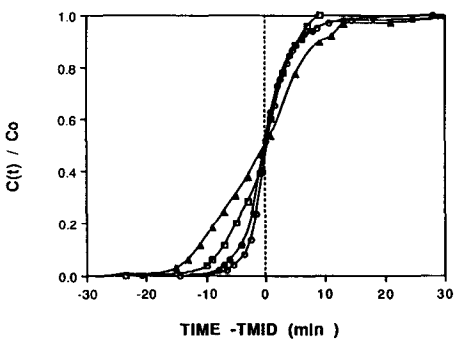

Fig. 5. Experimental breakthrough curves for the adsorption of HSA to DEAE Trisacryl M, showing the influence of bed length. The time is taken from the moment when enough liquid has passed through to displace the column dead volume and TMID corresponds to the time at 50% breakthrough, the midpoint. ○ = 1.4 cm; ● = 2.3 cm; □ = 2.7 cm; ▲ = 4.5 cm; – – – = ideal.

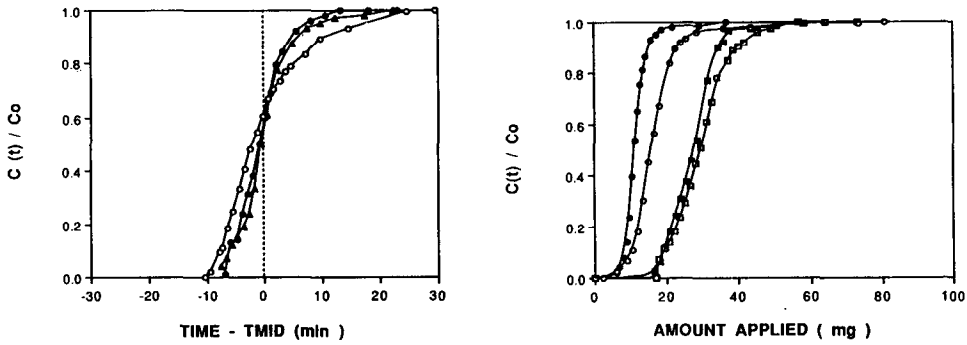

Fig. 6. Experimental breakthrough curves for the adsorption of HSA to DEAE Trisacryl M, showing the influence of temperature. z = 1.3 cm. ○ = 4°C; ● = 25°C; ▲ = 60°C and − − − = ideal.

Fig. 7. Experimental breakthrough curves for the adsorption of HSA to DEAE Trisacryl M, showing the influence of concentration at two different lengths. ■ = 1.5 mg/ml and 4.5 cm; □ = 3.0 mg/ml and 4.5 cm; ● = 1.5 mg/ml and 1.4 cm; ○ = 3.0 mg/ml and 1.4 cm.

greater the likelihood that the column is better packed and an even flow established throughout the bed, allowing a better performance. Further experiments with non-interactive low molecular solutes acting as probes could have been used to confirm this result.

A sharper breakthrough at the initial stage is also obtained at higher temperatures as illustrated by the profiles for the adsorption of HSA to DEAE Trisacryl M in Fig. 6. At high temperatures the protein solution is less viscous so that fluid mixing within the bed is superior. A similar trend with temperature was found when HSA was loaded onto a column packed with DEAE Sepharose FF (results not shown). The influence of the feed concentration is illustrated in Fig. 7, using the adsorption of HSA to DEAE Trisacryl M as an example. Slightly more distortion of the breakthrough curve is evident at higher concentrations, and this might be attributed to a decrease in the diffusion of the protein in solution. Mathematical simulations [30] of the adsorption of protein solution onto non-porous particles, using

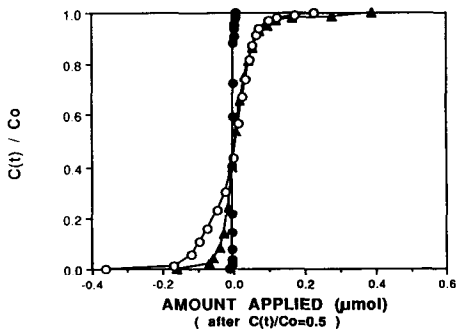

Fig. 8. Experimental breakthrough curves for the adsorption of different proteins to DEAE Trisacryl M, showing the influence of protein size. C_0 = 1.5 mg/ml for HSA (▲) and transferrin (○) (pH = 7.0), C_0 = 0.1 mg/ml for ferritin (●), z = 1.8 cm.

modifications of eqns. 1 and 3, have demonstrated that with this type of sorbent there is no change in the shape of the breakthrough curve for increasing protein concentration. From these simulations and the experimental results it can be concluded that the trend shown in Fig. 7 may be due to an increase in the restriction of movement of protein into the pores. This result was investigated further in terms of the model equation of Arnold *et al.* [8] and Arve and Liapis [16], as discussed later.

The effect of the protein size on packed bed adsorption was investigated using HSA, transferrin and ferritin and DEAE Trisacryl M. The experimental profiles in Fig. 8 represent the effluent concentration of the three proteins with respect to the amount of protein applied to the column. The curves were matched at the midpoint ($C(t)/C_0 = 0.5$) to standardize the different concentration used. ($C_0 = 1.5$ mg/ml for HSA and transferrin, whilst $C_0 = 0.1$ mg/ml for ferritin). A comparison of the curves of Fig. 8 leads to the conclusion that the largest protein, ferritin has the sharpest front, which is contrary to what one would expect, since one might anticipate that the slow diffusion of the large protein would render slow kinetics and a shallow curve. In addition, high values of the rate constants obtained for the experimental breakthrough curves of ferritin adsorbing to DEAE Trisacryl M were calculated, see Table IV, which corresponds to the sharp front of Fig. 8. The extremely small value for the capacity, $q_m = 0.003$ μmol/ml, suggests that ferritin may only bind to the external surface of the

TABLE I

COMPARISON OF LENGTH, TEMPERATURE AND CONCENTRATION ON THE SPREAD OF THE BREAKTHROUGH CURVE, ($V_{10} - V_{90}$) AND THE AMOUNT BOUND (OPERATING CAPACITY, q^*)

Resin[a]	Length (cm)	Temperature (°C)	Concentration (mg/ml)	$V_{10} - V_{90}$ (ml)	Capacity, q^* (mg/ml)
Trisacryl M	1.1			5.3	34
	1.3			6.8	45
	1.6			4.4	36
	2.3			5.3	36
	2.7			6.6	32
	4.5			10.5	31
Trisacryl M		4		9.4[b]	31[c]
		25		6.1	35
		60		6.1	39
Sepharose FF		4		8.8	36
		10		9.6	38
		25		6.4	43
		38		6.9	45
Trisacryl M			1.5[d]	4.4	36
			3.0	4.3	50
			1.5[e]	10.5	32
			3.0	13.0	33

[a] HSA adsorption.
[b] Standard deviation 20–30%.
[c] Standard deviation 5–17%.
[d] 1.4 cm column length.
[e] 4.5 cm column length.

sorbent particles. If this is the case, there is no slow diffusion into the pores, so that the overall rate, reflected in the value of k_1, becomes fast.

The change in the sigmoidal pattern of the breakthrough curves of Figs. 5–8 has been assessed from the values of $V_{10} - V_{90}$. As noted in the Introduction, large $V_{10} - V_{90}$ values represent large deviations from ideal, equilibrium behaviour. Table I, compares the $V_{10} - V_{90}$ values obtained from the breakthrough curves of HSA adsorbing to DEAE Sepharose FF for different bed lengths, temperatures and feed concentration. Although there is some experimental scatter amongst the values, it is clearly evident that short columns (1–2 cm bed heights) have low $V_{10} - V_{90}$ values whilst those for long columns (4–5 cm bed heights) are two-fold higher. This trend was also seen for the DEAE Sepharose FF studied (data not shown). Similarly, the $V_{10} - V_{90}$ values for adsorption to DEAE Trisacryl at 4°C is higher than at 60°C, and the $V_{10} - V_{90}$ values for the adsorption to DEAE Sepharose FF at 4°C is higher than at 38°C. These results emphasize what can be seen visually, that short columns and high operating temperatures exhibit relatively sharper breakthrough curves and hence have smaller $V_{10} - V_{90}$ values. A useful evaluation of the sigmoidal characteristic of a profile can therefore be carried out using this type of measurement.

The operating capacities, q^*, represented in the curves of Figs. 5–7 were derived using eqn. 1, and these capacities are also listed in Table I. There was found to be a general decline in capacity with increasing column length and decreasing temperature for both the DEAE Trisacryl M and the DEAE Sepharose FF. Again, these results for the capacities concur with the conclusions drawn from visual examination and the $V_{10} - V_{90}$ values. The more efficient short columns bind more protein possibly due to better bed packing ensuring superior flow patterns within the bed, and less channeling. In addition, the short columns are less likely to undergo bed compression, which invariably leads to a loss in operating capacity. High operating temperatures also exhibit a higher efficiency and greater capacity, because of an inherently lower fluid viscosity, better mixing and mass transfer.

Kinetic parameter evaluation

To use the model equations of Arve and Liapis [16], it is necessary to know *a priori* the association constant, K_a, since this value is directly related to the forward rate of interaction through the dynamic relationship, $K_a = k_1/k_2$. The K_a values used for the purpose of these investigations were those obtained from batch experiments previously reported [28]. It was found that the value of K_a could be changed by 20% without affecting the shape of position of the breakthrough curves obtained from theoretical simulations. (This was also the case with the film mass transfer coefficient, K_f). Thus the values for K_a obtained from the batch experiments were assumed to be adequate estimates of the appropriate values of K_a for the column experiments. Note however, that the maximum capacities given in Tables I and IV are lower than those reported in our earlier studies on batch adsorption [28] because the pH of the buffer used in the column experiments was 2 pH units less than in the batch experiments. This may have an effect on the overall charge of the protein which may affect how much binds to the sorbent. It has also been well established that there is a reduction in capacity when fixed bed chromatography is used as opposed to batch adsorption [31,32]. This loss could be attributed to bed compression and an increase in the film layer surrounding the resin. Both these effects will lead to a decrease in the transfer of the protein from solution to the adsorbent.

Using the models of Hubble [6], Thomas [7] and Arve and Liapis [16], the interaction rate constant, k_1, and the maximum capacity, q_m, were obtained by fitting iteratively the theoretical curve to the experimental breakthrough curve. Because of long computational times, the number of curves analysed using the model of Arve and Liapis was limited. In all cases, the maximum capacity for use in the theoretical solutions was changed to align the theoretical curve with the experimental one at the midpoint [$C(t)/C_0 = 0.5$]. In all cases it was necessary to change the value of k_1 or D_p from initial estimates to give curves of best fit, as determined by a least squares determination. A typical comparison of the theoretically determined profile and the experimental one is given in Fig. 9. The models of Hubble and Thomas yield very similar curves that correlate well with the experimental curve, and the resultant rate constants are similar. This result is to be expected since the assumptions inherent in the models of Hubble and Thomas are the same, although the method of numerical solution is different. The theoretical curve of Arve and Liapis fits the experimental curve well up to 50% breakthrough, and then the theoretical and experimental curves diverge towards the saturation point. This discrepancy between the theoretical and experimental curve at the later stages of the breakthrough curve has been shown to occur for several other model simulations [30,33]. It has been suggested that this divergence is due to the presence of non-specific binding on the adsorbent or conformational changes of the protein, two non-ideal occurrences that have not been accommodated in the models developed to date [16,18]. The worst curve fit of our experimental data was obtained with the model of Arnold *et al.*, the theoretical curve being a square root function, rather than a sigmoid (again see Fig. 9). This suggests that this model is not suitable for predicting the adsorption process of the proteins ferritin, HSA and transferrin to the weak ion-exchange resins, Trisacryl M and Sepharose FF, although it has gained some success in amino acid adsorption studies [8].

Fig. 10 shows the rate constants obtained from the models of Hubble and

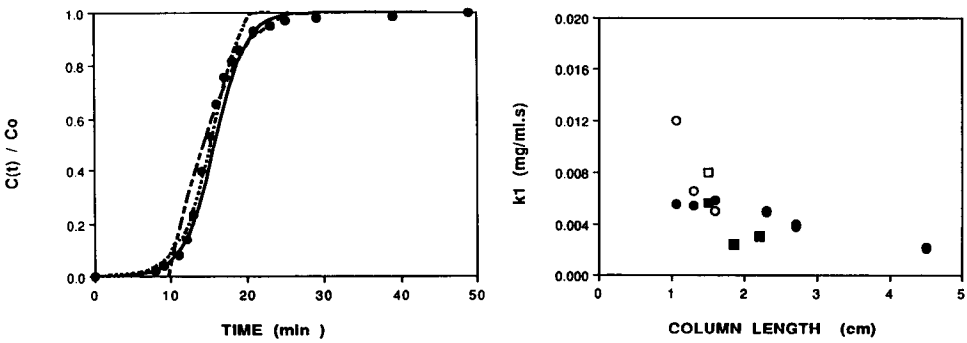

Fig. 9. Typical curve fit of the theoretical curves generated from Thomas (eqn. 3) (———), Arnold *et al.* (eqn. 4) (— — —) and Arve and Liapis (eqn. 5) (-------) to the experimental curve (●) of HSA adsorbing to DEAE Trisacryl M. C_0 = 1.5 mg/ml, q_m = 42 mg/ml resin, K_a = 56 ml/mg, u_0 = 0.042 cm/s, z = 1.3 cm, $K_f = 8 \cdot 10^{-6}$ m/s.

Fig. 10. Variation of the rate constant with the bed length, from the experiments with HSA adsorbing to DEAE Trisacryl M or DEAE Sepharose FF. The values for k_1 were obtained from the models of Hubble and Thomas. ○ = Hubble, Trisacryl; ● = Thomas, Trisacryl; □ = Hubble, Sepharose and ■ = Thomas, Sepharose.

TABLE II

THE EFFECT OF THE LENGTH OF THE PACKED BED AND OPERATING TEMPERATURE ON THE INTERACTION RATE CONSTANT, k_1, AS CALCULATED FROM THE THEORETICAL MODELS

Resin[a]	Length (cm)	Temperature (°C)	k_1^b	k_1^c (ml/mg s)	k_1^d
Trisacryl M	1.3	20	0.010	0.005	0.040
	4.5	20	0.002	0.002	0.005
Trisacryl M	1.3	4	–[e]	0.004[f]	–[e]
	1.3	60	–[e]	0.006	–[e]

[a] HSA adsorption.
[b] Eqn. 2 (Hubble).
[c] Eqn. 3 (Thomas).
[d] Eqn. 5 (Arve and Liapis).
[e] Not determined.
[f] Relative standard deviation 17%.

Thomas for the various column lengths. Other results of k_1 are given in Table II. The values of these rate constants are within the same order of magnitude as those calculated in our previous batch experiments [28], for example, $k_1 = 0.007$–0.012 ml/mg s for HSA adsorbing to DEAE Trisacryl M, pH 6.0. These results obtained from the Hubble or Thomas models indicate a trend of increasing k_1, with decreasing column length, for example, when $z = 1.3$ cm $k_1 = 0.012$ ml/mg s, whilst at $z = 4.5$ cm $k_1 = 0.002$ ml/mg s. The interaction rate, k_1, is indicative of the interaction of a particular protein with the functional groups on the resin, and should therefore remain constant for increasing column lengths. These observations suggest that the rate constants, k_1, derived from the Hubble and Thomas models are lumped constants, which incorporate but not discriminate other mass transfer resistances such as protein diffusivities, or pore resistances. Table II also shows that there is a slight increase of k_1 with temperature, and when considering the form of the Arrhenius relationship, $k_1 = Ae^{-Ea/RT}$, which suggests that at higher temperatures the likelihood of interaction is

TABLE III

THE EFFECT OF THE LENGTH OF THE PACKED BED AND OPERATING TEMPERATURE ON THE EFFECTIVE DIFFUSIVITY, D_p, AS CALCULATED FROM THE THEORETICAL MODELS

Resin[a]	Length (cm)	Temperature (°C)	D_p^b ($\cdot 10^{-11}$ m/s)	D_p^c
Trisacryl M	1.3	20	1.10	6.1
	4.5	20	0.28	6.1
Trisacryl M	1.3	4	0.39	6.1
	1.3	60	0.91	6.1

[a] HSA adsorption.
[b] Eqn. 4 (Arnold *et al.*).
[c] Eqn. 5 (Arve and Liapis).

TABLE IV

THE INFLUENCE OF PROTEIN SIZE ON THE INTERACTION RATE, AS CALCULATED FROM THE THEORETICAL MODELS

Protein[a]	q_m (μmol/ml)	k_1[b] (ml/μmol s)	k_1[c]	D_p[d] ($\cdot 10^{-11}$ m^2/s)
Human Serum Albumin	1.49[e]	0.12	0.10	0.7
Transferrin	0.98	0.13	0.25	1.1
Ferritin	0.003	4.51	5.14	1.1

[a] Adsorption to DEAE Trisacryl M.
[b] Eqn. 2 (Hubble).
[c] Eqn. 3 (Thomas).
[d] Eqn. 4 (Arnold *et al.*).
[e] Buffer pH 7.0.

greater since more molecules will have higher energy, this increase is not surprising. Table III shows the effect of column length and operating temperature on the effective diffusivity, D_p, as calculated from theoretical models. The results obtained from the model of Arnold *et al.* [8] show a trend of increasing D_p with decreasing column length, and increasing operating temperature, which is similar to the effect on k_1 in the model values in Table II. The fact that D_p is actually a lumped parameter of Arnold *et al.* may explain this similarity.

In order to determine the effect of pore-to-protein size on the breakthrough curves, the adsorption of ferritin, transferrin and HSA to the DEAE Trisacryl M were examined in independent experiments. Table IV lists the operating capacities, q_m, the interaction rates, k_1 (from eqns. 2 and 3) and the effective diffusivities (from eqn. 4) for the three proteins adsorbing to DEAE Trisacryl M. Considering the differences in the hydrodynamic radii of the three proteins (diameter of ferritin is about 110 Å, whilst that of HSA is 45 Å) according to the correlation of Young *et al.* [21], the diffusion of ferritin into the pores of the DEAE Trisacryl M is anticipated to be significantly slower than transferrin or HSA. This behaviour in fact was observed with the capacity of DEAE Trisacryl M for ferritin being small, 0.003 μmol/ml, compared to HSA, 1.49 μmol/ml, due to these geometric constraints. Moreover, it is conceivable that adsorption of ferritin is limited to the surface of the adsorbent. Experimental capacities for the adsorption of several other proteins, varying in molecular weights onto the cation-exchange resin, Whatman Cellulose CM52, have also shown that capacity decreases with increasing molecular weight of a protein [34].

Note however, that the effective diffusivities shown in Tables III and IV are not significantly smaller than the correlated diffusivities of the proteins in free solution [35] although the model of Arnold *et al.* which has been used to calculate these values for D_p, neglects all the other mass transfer resistances associated with adsorption. Furthermore, the correlation between the theoretical curves of eqn. 4 and the experimental curves was very poor, so that the values obtained should be treated with certain scepticism.

The values for k_1, from eqn. 2, also appear protein dependent, see Table IV, with the highest value being for the largest protein ferritin. As k_1 is protein specific, this difference is not surprising, and similar high values were calculated in our bath

experiments. Furthermore, this concurs with the relative steepness of the breakthrough curves of Fig. 8, where the largest protein appeared to have the sharpest front.

These results highlight the necessity for theoretical models to reflect the physical features of the adsorption process if the derived rate constants are to have physical significance.

CONCLUSIONS

In this investigation, the column length, temperature, protein concentration and protein size have been varied to assess their influence on the capacity of ion-exchange resins and on the kinetic parameters associated with an ion-exchange adsorption interaction. Improved performance, in terms of a higher operating capacity and sharper breakthrough curves, was seen on shorter columns. This observation has been well known [20] in large-scale process chromatography where difficulties in packing have been overcome by the design and implementation of "stacked" bed columns. An increase in the temperature of the operation was also found to improve the performance. Whilst many proteins are heat-sensitive, restricting the temperature of the purification steps to 4–10°C, there are proteins, for example HSA, which are stable at temperatures of up to 60°C. Operation at higher temperatures thus looks promising in terms of increased adsorbent capacity and better fluid characteristics. A two-fold increase in the protein concentration of the feed had little influence on the shape of the breakthrough curve. This observation is important from a process aspect, because it implies that a variation on the feedstock concentration, for example the HSA content in plasma, will not unduely affect the performance. As an added bonus, an increase in the feedstock concentration will reduce the processing time. The results from the breakthrough curves of different proteins, reveal that the capacity of the ion-exchange resin, DEAE Trisacryl M is smallest for the largest protein, ferritin, although the large values obtained from the mathematical models for the diffusivities suggests that this diffusion is surface related, and in fact ferritin adsorption is limited to the exterior of the adsorbent.

The application of the mathematical models used in these investigations has shown that there are still shortcomings in these models as projected in the Theory section. That there is a need to develop further the concept of a "modus", a physical model that reflects the realities of the adsorption process is undoubtable. Evidence of non-idealites are apparent in the experimental breakthrough curves and these deviations from ideal behaviour are as yet unquantifiable using the mathematical solutions available today.

ACKNOWLEDGEMENTS

The support of the Australian Research Grants Committee and Monash University Research Committee is grately acknowledged.

REFERENCES

1 F. B. Anspach, A. Johnston, H.-J. Wirth, K. K. Unger and M. T. W. Hearn, *J. Chromatogr.*, 499 (1990) 103.
2 A. J. P. Martin and R. L. M. Synge, *Biochem. J.*, 35 (1941) 1351.
3 E. Gleukauf, *Trans. Faraday Soc.*, 51 (1955) 34.
4 S. Yamamoto, M. Nomura and Y. Sano, *AIChE. J.*, 33 (1987) 1427.
5 S. Golshan-Shirazi and G. Guiochon, *J. Chromatogr.*, 506 (1990) 495.
6 J. Hubble, *Biotech. Tech.*, 3 (1989) 113.
7 H. C. Thomas, *Am. Phys. Chem. Soc. J.*, 66 (1944) 1664.
8 F. H. Arnold, H. W. Blanche and C. R. Wilke, *Chem. Eng. J.*, 30 (1985) B9.
9 T. Vermeulen, *Ind. Eng. Chem.*, 45 (1953) 1664.
10 R. D. Jr. Fleck, D. J. Kirwan and K. R. Hall, *Ind. Eng. Chem. Fundam.*, 12 (1) (1973) 95.
11 S. Katoh, T. Kambayashi, T. R. Deguchi and F. Yoshida, *Biotechnol. Bioeng.*, 20 (1978) 267.
12 D. R. Garg and D. M. Ruthven, *Chem. Eng. Sci.*, 28 (1973) 791.
13 C. Tien and G. Thodos, *AIChE. J.*, 5 (1959) 373.
14 E. L. Morton and P. W. Murni, *AIChE. J.*, 13 (1967) 965.
15 C. R. Antonson and J. S. Dranoff, *Chem. Eng. Progr. Symp. Ser.*, 96 (1969) 65.
16 B. H. Arve and A. I. Liapis, *Biotechnol. Bioeng.*, 32 (1988) 616.
17 D. M. Ruthven, *Principles of Adsorption and Adsorption Process*, Wiley, New York, 1984, pp. 261–268.
18 M. A. McCoy and A. I. Liapis, *J. Chromatogr.*, 548 (1991) 25.
19 J. R. Sportsmann, J. D. Liddell and G. S. Wilson, *Anal. Chem.*, 55 (1983) 771.
20 J.-Ch. Janson and P. Hedman, *Adv. Biochem. Eng.*, 25 (1982) 45.
21 M. E. Young, P. A. Carroad and R. L. Bell, *Biotechnol. Bioeng.*, 12 (1980) 947.
22 C. R. Davies, P. S. Malchesky and G. M. Saidel, *Artificial Organs*, 14 (1990) 14.
23 S. Ghodbane and G. Guiochon, *J. Chromatogr.*, 452 (1988) 209.
24 J. H. Know and H. M. Pyper, *J. Chromatogr.*, 363 (1986) 1.
25 I. Lundstrom and H. Elwing, *J. Theor. Biol.*, 110 (1984) 195.
26 J. H. Petropoulos, A. I. Liapis, N. P. Kolliopoulos, J. K. Petrou and N. K. Kanellopoulos, *Bioseparations*, 1 (1990) 69.
27 A. Johnston and M. T. W. Hearn, *J. Chromatogr.*, 512 (1990) 101.
28 A. Johnston and M. T. W. Hearn, *J. Chromatogr.*, 556 (1991) in press.
29 H. Ohashi, T. Sugawar, K. Kikuchi and K. Konno, *J. Chem. Eng. Japan*, 14 (1981) 433.
30 Q. M. Mao, A. Johnston, I. G. Prince and M. T. W. Hearn, *J. Chromatogr.*, 548 (1991) 147.
31 A. Johnston, *M.Sc. Thesis*, Monash University, Melbourne, 1988.
32 K. K. Unger and R. Janzen, *J. Chromatogr.*, 373 (1986) 227.
33 B. J. Horstmann and H. A. Chase, *Chem. Eng. Res. Des.*, 67 (1989) 243.
34 R. K. Scopes, *Anal. Biochem.*, 114 (1981) 8.
35 P. A. Davies, *J. Chromatogr.*, 483 (1989) 221.
36 M. T. W. Hearn, A. H. Hodder, F. W. Fang and M. I. Aguilar, *J. Chromatogr.*, 548 (1991) 117.